

# Cap-hardening parameters of Cam-clay model variations with soil moisture content and shape-restricted regression model

Mehari Z. Tekeste<sup>1\*</sup>, Desale H. Habtzghi<sup>2</sup>, A. Jos Koolen, Jr.<sup>3</sup>

(1. John Deere Technology Center, Moline, IL, 61265, USA;

2. Department of Statistics, The University of Akron, Akron, OH 44325, USA;

3. Soil Technology Group, Wageningen University, Bomenweg 4, 6703 HD Wageningen The Netherlands)

**Abstract:** Modeling of soil elastic and permanent plastic volumetric strains (compaction) caused by loading from machinery vehicles using the modified Cam-clay soil constitutive model requires understanding the behaviors of compression and rebound parameters under unsaturated soil conditions. Oedometer tests were conducted on a sandy loam, a loam, and a clay loam soil, all tropical soils, at three initial soil moisture contents and five maximum stress levels (50, 100, 200, 300 and 400 kPa). The objectives were to investigate the effects of soil moisture content and maximum applied stress on the modified compression index ( $\lambda^*$ ) and modified rebound index ( $\kappa^*$ ) parameters of a modified Cam-clay soil model on the three soils and predict the compressibility indices using the shape-restricted modeling technique. The clay loam soil showed higher compressibility at lower maximum stress levels and wet moisture conditions (-10 kPa soil moisture potential) but as the maximum applied stress increased (> 200 kPa), the modified compression index ( $\lambda^*$ ) variations with soil moisture content were insignificant ( $p > 0.05$ ). A loam soil exhibited similar compression characteristics to a clay loam soil at 26.12% d.b. and 23.67% d.b., respectively. For a sandy loam soil, both critical state parameters were less sensitive to the variations in soil moisture content. The loam soil, which had an organic matter content of 6.33%, rebounded more than clay loam and sandy loam soils especially at higher applied stress values. On average, the modified compression index ( $\lambda^*$ ) was about 23 to 36 times the modified rebound index ( $\kappa^*$ ). Shape-restricted and quadratic model fittings are presented to explain the relationship between the critical state parameters and maximum applied stresses for each soil moisture content. The model fitting results indicated that shape-restricted regression predicted the modified Cam-clay model parameters as a function of maximum applied stress (or pre-compression stress) at very low Average Squared Error Loss (ASEL) and did so better than parametric quadratic equations.

**Keywords:** modified compression index ( $\lambda^*$ ), modified rebound index ( $\kappa^*$ ), axial stress, uniaxial compression cyclic test, soil moisture, soil types

**Citation:** Tekeste, M. Z., D. H. Habtzghi, and A. J. Koolen, Jr. 2013. Cap-hardening parameters of Cam-clay model variations with soil moisture content and shape-restricted regression model. *Agric Eng Int: CIGR Journal*, 15(2): 10–24.

## 1 Introduction

Soil compaction is an important soil process that modifies soil permeability to air and water, soil strength and root penetrability (Al-Adawi and Reeder, 1996; Hillel,

1998). Excessive soil compaction commonly occurs when the external loading exceeds the pre-compression soil stress or loading on compactable soil conditions (Wiermann et al., 2000; and Raper, 2005). Previous studies have indicated that crop production and the environment are negatively affected by excessive soil compaction (Radcliffe et al., 1989; Soane and van Ouwerkerk, 1994; Hamza and Anderson, 2005; Raper, 2005). Soil stresses from external loading exceeding internal soil structure strength can result in deeper and long-lasting subsoil compaction (Wiermann et al., 2000).

**Received date:** 2012-08-16 **Accepted date:** 2013-04-03

\* **Corresponding author:** Mehari Z. Tekeste, Former Graduate Student of Soil Technology Group, Wageningen University, Bomenweg 4, 6703 HD Wageningen, The Netherlands. Current Address: John Deere Technology Center, Moline, IL, 61265. Email: [tekestemehari@johndeere.com](mailto:tekestemehari@johndeere.com).

Remediation of subsoil compaction is often energy intensive, and for low organic matter sandy soils, the benefits are not necessarily sustainable since the soil reconstitutes to the compacted state quickly (Van den Akker et al., 2003; Raper, 2005). In highly modernized agriculture, supplemental inputs such as drainage, intensive fertilization and irrigation can compensate the detrimental effects of compaction on crop production (Van den Akker et al., 2003). Soil compaction problems are still of concern with the continuously increasing trends in vehicle weight; and continuous need for trafficking on weakly structured (less than 5-mm soil aggregates) and wet soil moisture state (plastic to swelling limit range) soil conditions for instance during seed-bed preparation and harvesting underground roots (Poodt et al., 2003). The size of tractors currently used in less modernized agriculture such as in tropical regions of the globe may be relatively small, however, with trafficking on compaction-prone low organic matter and erodible tropical soils, repeated wheel passes, limited expensive inputs in the form of deep tillage, drainage, fertilization and irrigation, the magnitude of soil degradation from compaction is significant (Lal, 1994; Soane and van Ouwerkerk, 1994).

Numerical modeling tools such as the finite element method are now becoming useful tools in soil compaction management from wheeling to reduce or prevent soil quality deterioration (Van den Akker et al., 2003). The computational modeling can provide useful and relatively quick information to farm managers, soil protection environmental regulatory agencies, and manufacturers of tire and soil-engaging equipment.

With the availability of powerful computers and recent advances in adaptive meshing for large-geometric deformations of elements, explicit numerical solvers and representative boundary constraints (ABAQUS, 2004), the finite element method is a good tool for simulating tire-soil and machine-soil interactions (Fielke, 1999; Mouazen and Neményi, 1999; Upadhyaya et al., 2002). Poodt et al. (2003) modeled tire-soil using PLAXIS finite element code (Plaxis bv, Delft, The Netherlands) to predict cap-plasticity compaction zones in soil from a wide range of vertical tire load and inflation pressure

combinations (8 - 12 Mg vertical tire load and 100 - 289 kPa inflation pressure) common in sugar beet harvesters. Poodt et al. (2003) used stress-strain data from the uniaxial compression tests of Lobith fluvial loam soil to determine Cam-clay soil model parameters. The cap-plasticity zones in the soil model were obtained where finite element-predicted vertical stress exceeded the measured pre-consolidation stress. The finite element method predicted stresses that were less than the pre-compression values. Chiroux et al. (2005) modeled a loaded rolling rigid wheel (5.8 and 11.6 kN vertical load) using the Drucker – Prager soil model with ‘cap’ plasticity and ‘cap’ hardening parameters in finite element code of ABAQUS/Explicit (Dassault Systèmes Americas Corp., Waltham, Mass., USA). The finite element model under-predicted the wheel rut depth (compaction) for the 11.6 kN vertical wheel load as compared to the experimental data.

The fidelity of finite element modeling on agricultural soils is highly dependent on the availability of versatile soil constitutive models that account for heterogeneous and unsaturated soil conditions (Bailey and Johnson, 1996; Wulfsohn and Adams, 2002). Good soil constitutive models that account for variations in soil condition can improve the prediction soil responses from general vehicle loading for various tire and wheel characteristics, including vertical load, tire size, and tire inflation pressure.

### 1.1 Soil constitutive models

Soil constitutive models establish the relationship between applied stresses and strains. Material elastic, hardening law, yield criterion, and plastic potential parameters are required to mathematically formulate the soil constitutive relationships. Laboratory or field experiment tests such as uniaxial compression, triaxial, or shear box tests can be used to establish soil constitutive relationships. It is essential to select the appropriate material testing representative of initial soil conditions and to measure the dominant soil strain behavior under the stress state of soil-machine interaction problems.

The Cam-clay soil model, developed from critical state mechanics theory, successfully describes soil shear and volumetric behaviors upon normal and deviatoric

applied stresses (Wood, 1990). The cylindrical stress state ( $\sigma_2 = \sigma_3$ ) triaxial test on normally consolidated saturated and remolded clay soil (Roscoe et al., 1958) was used to develop the original Cam-clay model. The Cam-clay soil constitutive model uses three boundary equations and requires five constitutive soil parameters to explain the elastic behavior, Mohr-Coulomb, plastic hardening (soil compaction) and pre-consolidation stress.

The three critical state soil model equations are Normal Consolidation Line (NCL) for primary loading responses (Equation (1)) in mean normal stress ( $p$ ) vs. specific volume ( $v$ ); Unloading-Rebound Line (URL) for rebound or swell responses on the  $p$ - $v$  plane (Equation (2)); and Critical State Line (CSL) for the critical state failure on the  $p$ -deviatoric stress ( $q$ ) plane (Equation (3)) (Atkinson and Bransby, 1978).

**Normal Consolidation Line (NCL):** A straight line in the logarithmic scale of the compression plane  $v$  vs.  $\ln(p)$ , with  $q = 0$  and is given by:

$$v = v_\lambda - \lambda \ln(p) \quad (1)$$

**The Unloading/Rebound Line (URL):** Represents soil rebound or recovery after load removal:

$$v = v_\kappa - \kappa \ln(p) \quad (2)$$

**The Critical State Line (CSL) on the  $p$ - $q$  plane:** Represents the yield locus plane and is defined as:

$$q_{cs} = M p_{cs} \quad (3)$$

The slope parameter of CSL in the  $q$ - $p$  plane,  $M$ , is related to the angle of internal friction,  $\phi$ , of the Mohr-Coulomb failure criterion (Chen and Mizuno, 1990) according to:

$$M = \frac{6 \sin \phi}{3 - \sin \phi} \quad (4)$$

where,  $v$  = specific volume ( $v = 1/\rho$ ; where  $\rho$  is bulk density);  $v_\lambda$  = specific volume at  $p = p_o$  ( $p_o$  was considered 10 kPa) in NCL;  $\lambda$  = compression index (determines the compressibility of a soil in primary loading);  $v_\kappa$  = specific volume at  $p = p_o$  ( $p_o$  was considered 10 kPa) in URL;  $\kappa$  = rebound index (determines the rebound ability of a soil during unloading);  $\ln(p)$  = natural log of mean normal stress;  $p_{cs}$  = mean normal stress on critical state line;  $M$  = slope of the critical state line;  $q_{cs}$  = mean deviatoric stress on critical state line.

Mean normal stress ( $p$ ) and mean deviatoric stress ( $q$ ) are stress-invariants, where  $p = \frac{1}{3}(\sigma_1 + \sigma_2 + \sigma_3)$  ;

$$q = \frac{\sqrt{2}}{2} \left( \sqrt{(\sigma_1 - \sigma_2)^2 + (\sigma_2 - \sigma_3)^2 + (\sigma_3 - \sigma_1)^2} \right) \quad \text{and}$$

$\sigma_{i,i=1,2,3}$  are the major, intermediate and minor principal stress, respectively. For the cylindrical stress state where  $\sigma_2 = \sigma_3$ , the stress invariants can be simplified as  $p = \sigma_{oct} = \frac{1}{3}(\sigma_1 + 2\sigma_3)$  , and  $q = (\sigma_1 - \sigma_3) = \frac{3}{\sqrt{2}} \tau_{oct}$  , where  $\sigma_{oct}$  and  $\tau_{oct}$  are octahedral normal and shear stresses, respectively.

The Cam-clay material model with the ‘‘cap hardening’’ option has been integrated into finite element codes such as PLAXIS (Brinkgreve and Vermeer, 1998) and ABAQUS (ABAQUS, 2004). The quasi-empirical macro soil model of COMPSOIL (O’Sullivan et al., 1999; and Defosse et al., 2003) also utilizes the critical state soil parameters for soil compaction modeling. The modified Cam-clay soil model parameters needed in the PLAXIS material model (Brinkgreve and Vermeer, 1998) are Poisson’s ratio ( $\nu$ ), modified compression index ( $\lambda^*$ ), modified rebound index ( $\kappa^*$ ), cohesion ( $C$ ), angle of internal friction ( $\phi$ ), dilatancy angle ( $\psi$ ),  $K_o$ -parameter ( $K_o = M$ ) and pre-consolidation stress ( $\sigma_{pc}$ ).

## 1.2 Determination of soil compaction (hardening) model parameters

The major principal stress ( $\sigma_1$ ) is a dominant stress controlling compressive behavior of soils upon loading from wheels (Söhne, 1958; Koolen and Kuipers, 1983). Cyclic uniaxial compression tests on soil cores can sufficiently simulate soil response at tire-soil interaction under the major principal stress loading (Koolen, 1994) and may represent soil behaviors in contact with tires at least twice, for instance, between the tractor front and rear tires (O’Sullivan and Robertson, 1996). The primary loading up to a maximum applied stress level results in the soil volume compression that tends to partially recover during unloading. Numerous studies were conducted to determine critical state soil parameters using an oedometer, triaxial and shear box tests on laboratory remolded soil specimens (Petersen, 1993; O’Sullivan et al., 1996; Smith et al., 1996; Adams and

Wulfsohn, 1998) and on intact core samples from fields (O'Sullivan and Robertson, 1996; Kirby and O'Sullivan, 1997). The studies indicated that critical-state soil parameters for unsaturated agricultural soils varied by quality and preparation of soil specimens, soil moisture conditions and stress paths. Bailey and Johnson (1996) and Wulfsohn and Adams (2002) noted the challenges for accurate prediction of soil compaction behaviors on unsaturated soils are availability of less disturbed soil samples and tests that are less costly, simple and quick.

In our study, the modified compression index ( $\lambda^*$ ) and modified rebound index ( $\kappa^*$ ) parameters, as influenced by soil moisture and estimates from uniaxial compression tests were considered as most influential on the soil compaction behaviors. In this article, the modified compression index ( $\lambda^*$ ) and modified rebound index ( $\kappa^*$ ) are computed from the slope of the primary compression line ( $C_c$ ) and the slope of the unloading-rebound lines ( $C_s$ ) in graphs of void ratio,  $e$ , vs.  $\text{Log } \sigma_1$ , for uniaxial compression (oedometer) tests using Equations (5), (6) and (7) (Brinkgreve and Vermeer, 1998). The equations take into account the initial packing state expressed as initial void ratio and Poisson's ratio for the elastic behavior.

$$\lambda^* = \frac{C_c}{2.3 * (1 + e_o)} \quad (5)$$

$$C_c = \frac{e_2 - e_1}{\log\left(\frac{\sigma_2}{\sigma_1}\right)} \quad (6)$$

$$\kappa^* = 1.3 \times \frac{(1 - \nu)}{(1 + \nu)} \times \frac{(C_s)}{(1 + e_o)} \quad (7)$$

where,  $\lambda^*$  = Modified compression index;  $\kappa^*$  = Modified rebound index;  $\nu$  = Poisson's ratio;  $e_o$  = Initial void ratio;  $C_c$  = Slope of primary compression line;  $C_s$  = Slope of unloading-rebound line;  $e_1$  and  $e_2$  = Void ratios along the compression curve; and  $\sigma_1$  and  $\sigma_2$  = Stress values along the compression curve.

The formula used to estimate  $C_s$  is similar to that of  $C_c$  (Equation (6)) except the former uses void ratio ( $e$ ) and log-stress ( $\sigma$ ) values from the rebound curve of the oedometer test data. Poisson's ratio ( $\nu$ ), an elastic parameter, is important in the unloading phases. Its

value usually ranges between 0.1 and 0.2. A Poisson's ratio of  $\nu = 0.2$  was assumed after Poodt et al. (2003) for modeling agricultural soils. Initial void ratio values ( $e_o$ ) were obtained from the void ratio at the pre-load stress (10 kPa) of the oedometer tests that vary with soil type, soil moisture content and maximum principal stress.

Studies of the variability of the modified Cam-clay model parameters under a wide range of soil moisture contents and loading magnitudes on tropical soils are limited. Besides utilizing simple tests to determine the soil mechanical parameters, surface response models trained from scattered test data are needed to quickly generate soil model parameters for unsaturated soils. Once validated from test data, the surface response models can be looped into an inverse optimization process flow with finite element analysis solvers and can be used to further train the soil model parameters to improve simulation-based support of soil-wheel interaction problems. Based on previous studies and empirical inspection of the relationship of the Cam-clay model parameters and soil moisture, the implementation of a non-parametric shape-restricted regression model was investigated for agricultural tropical soils.

### 1.3 Objectives

The main objectives of the study were: 1) to determine the modified compression ( $\lambda^*$ ) and rebound ( $\kappa^*$ ) indices of the Cam-clay soil model on clay loam, loam and sandy loam for unsaturated soil conditions; 2) to investigate the effects of soil type, moisture content and maximum axial stress levels on the modified compression ( $\lambda^*$ ) and rebound ( $\kappa^*$ ) indices; and 3) to introduce a nonparametric regression model to predict the modified compression ( $\lambda^*$ ) and rebound ( $\kappa^*$ ) indices.

## 2 Materials and methods

### 2.1 Soil characterization

Soil samples for oedometer tests were collected from three agro-ecological zones in Eritrea, namely the central highland (21°28' 30.62" N 49°50' 42.22" E), the western lowland (15°47' 00.00" N 38°27' 00.22" E), and the coastal plains (15°48' 55.83" N 39°04' 15.87" E) (Tekeste, 1999). According to FAO-soil classification (FAO-UNESCO, 1988), the dominant soils in the central

highland, western lowland and coastal plains are classified as *Lixisols*, *Leotosols*, and *Fluvisols*, respectively. The soils physical and chemical properties

including particle size distribution, organic matter content, soil acidity (pH), calcium carbonate, particle density and soil moisture retention information are given in Table 1.

**Table 1 Soil physical and chemical properties from soil sampling sites at central highland, coastal plains and western lowland zones**

Site Name	Particle density /g cm <sup>-3</sup>	Soil moisture content (-10 kPa soil moisture potential)/% d.b.	Particle size distribution <sup>1</sup>			Textural class <sup>2</sup>	Organic matter/%	Soil pH (1:2.5 KCl) <sup>3</sup>	CaCO <sub>3</sub> /%
			S/%	Si/%	C/%				
Central highland	2.81	34.00	26.68	37.84	35.48	CL	5.59	6.03	0.31
Coastal plains	2.76	33.82	41.23	38.92	19.84	L	6.33	7.6	0.24
Western lowland	2.72	14.09	68.69	11.7	19.61	SL	2.22	6.98	0.88

Note: <sup>1</sup> S - sand fraction, Si - silt fraction, C - clay fraction; <sup>2</sup> CL - Clay Loam, L - Loam, SL - Sandy Loam; <sup>3</sup> Soil pH was measured in potassium chloride (KCl) soil solution 1:2.5 water: KCl ratio.

## 2.2 Experimental design

The oedometer testing experiment was arranged using a split-plot factorial design with three replicates. The soil type was considered as the experimental block, each having three moisture levels as the main plot treatments, and five maximum stress levels as the subplot treatments. For each soil type, the remolded soil samples (5-mm sieved aggregates) were uniaxially compressed from pre-load stress to five maximum stress levels. Three soil moisture levels, five maximum stress levels, and three replications (3 × 5 × 3) gave 45 tests for each of the three soils.

## 2.3 Uniaxial soil sample preparation

Soil samples were prepared into three soil moisture levels representing typical field soil moisture conditions occurring during field operations, starting from a plastic soil state. Soil samples sieved through 5 mm were first brought to a soil moisture potential of -10 kPa using a sandbox apparatus (Eijkelpkamp Agrisearch Equipment, Giesbeek, the Netherlands).

The three soil moisture levels were prepared according to the following criteria: soil moisture level – 1 (“wet”): SM<sub>-10 kPa</sub>; soil moisture level – 2 (“moist”): SM<sub>air dry</sub> + (5/6) (SM<sub>-10 kPa</sub> - SM<sub>air dry</sub>); and soil moisture level – 3 (“drier”): SM<sub>air dry</sub> + (2/3) (SM<sub>-10 kPa</sub> - SM<sub>air dry</sub>). Soil samples from the sandbox apparatus at soil moisture potential of -10kPa were oven-dried for 24 hrs at 105°C to determine the soil moisture content (SM<sub>-10 kPa</sub>). Soil samples at -10 kPa soil moisture potential were air-dried to prepare samples for the soil moisture level - 2 (“moist”) and soil moisture level - 3 (“drier”).

## 2.4 Uniaxial compression test

The uniaxial compression or oedometer test is an easy and a fast method to obtain stress and strain data on agricultural soils for modeling soil compaction (Koolen, 1974). In the uniaxial compression test, a vertical uniaxial stress was applied using axial loading of a cylindrical piston and the soil volume compresses in the axial direction with increasing stress until the pre-selected maximum stress level was reached. The loading piston moving direction was then reversed allowing the soil volume to rebound (swell). The cylinder containing the soil was rigid, so there were no strains in the horizontal direction.

Soil samples from the three soil moisture levels were filled into metal cylinders (7.5 cm in diameter and 5 cm in height) and subjected to cyclic (loading-reloading) uniaxial compression loading using a material testing machine (Zwick model 1455 material testing machine (Zwick GmbH and Co. KG, Ulm, Germany)). The parameters of pre-load stress, lowest reversal stress point, highest reversal stress point (maximum stress), sampling frequency and test speed were defined in the control unit of the material testing machine. Normal stress-strain primary compression data were collected using a pre-load stress value of 10 kPa and increasing to the highest reversal stress (maximum stress) values. Data for the rebound line (strain recovery displacement-force data) were collected by decreasing from the highest reversal stress to the lowest stress point (5 kPa). The compression speed was 0.5 mm s<sup>-1</sup>. The displacement and force data were recorded at a frequency of 50 Hz.

For each uniaxial compression test, the sample height was measured at the preload stress (10 kPa) to compute initial void ratio values ( $e_o$ ) for the modified compression index ( $\lambda^*$ ) and rebound index ( $\kappa^*$ ) computations.

2.4.1 Determination of critical state soil model parameters: Modified compression index ( $\lambda^*$ ) and rebound index ( $\kappa^*$ )

The slope of the normal compression and reloading lines from each run were determined from the graphs of

log stress vs. void ratio referring to  $C_c$  and  $C_s$ , respectively. Then the modified compression index ( $\lambda^*$ ) and modified rebound index ( $\kappa^*$ ) were derived using Equations (10) and (11). A Poisson's ratio of 0.2 and initial void ratio values at pre-load stress (Table 2) were used to convert the  $C_c$  and  $C_s$  to the modified compression index ( $\lambda^*$ ) and modified rebound index ( $\kappa^*$ ). A Poisson's ratio of 0.2 is typically used value in modeling agricultural soils (Poodt et al., 2003).

**Table 2 Values of initial void ratio ( $e_o$ ) measured at preload stress (-10 kPa) from the uniaxial compression test for clay loam, loam and sandy loam**

Clay Loam (CL)		Loam (L)		Sandy Loam (SL)	
Soil moisture content /% d.b.	Initial void ratio ( $e_o$ )	Soil moisture content /% d.b.	Initial void ratio ( $e_o$ )	Soil moisture content /% d.b.	Initial void ratio ( $e_o$ )
26.12	2.72	23.67	2.14	10.49	1.58
29.94	2.71	30.87	2.32	12.29	1.47
34.00	2.57	33.82	2.20	14.09	1.53

Once the mechanical parameters were determined, statistical analysis was done using PROC MIXED in SAS (SAS Institute Inc., Cary, NC, USA) with a significance level,  $\alpha = 0.05$ , and for all possible pairwise comparisons on the effects (soil moisture and maximum stress). Least squares means (LSMEANS) were used.

## 2.5 Curve fitting using nonparametric regression

In typical regression analysis, a straight line is fit to the data when the relationship between the response variable and a linear combination of the predictors is linear. Otherwise, polynomial, logarithmic or exponential regression is typically used to fit the data. In many situations when the underlying regression function or scatter plot has a particular shape or form, the fitted model can be characterized by certain order or shape restrictions, a shape-restricted class of regression function will be preferred. This regression method provides a flexible fit to the data and improves regression predictions. Detailed exposition of widely studied regression methods, particularly polynomial regression and shape-restricted regression are given in Weisberg (2005) and Robertson et al. (1988), respectively. Shape-restricted regression is a nonparametric approach for building models whose fits are monotone, convex or concave in their covariates. These assumptions are commonly applied in biology (Obozinski et al., 2008);

medicine (Schell and Singh, 1997); psychology (Kruskal, 1964); ranking (Zheng et al., 2008); statistics (Barlow and Brunk, 1972); and survival analysis (Meyer and Habtzghi, 2011).

Initial observation of uniaxial compression test data for different soil moisture conditions in our study indicated that the relationship between the modified compression and maximum applied stress levels; rebound index values and maximum applied stress levels have certain shapes. The shapes differ, depending on soil moisture content. In addition, from the scatter plots of Figures 1 and 2, there are some curvatures in the relationship between maximum applied stress and modified compression index ( $\lambda^*$ ), and maximum applied stress and modified rebound index ( $\kappa^*$ ) at different levels of soil moisture content. Use of shape-restricted regression seems appropriate for investigating the relationship between maximum applied stress and soil mechanical parameters. Previous studies also support the need to evaluate shape-based assumptions. For instance, O'Sullivan et al. (1999) observed quadratic forms of the relationship between slopes of NCL and soil moisture, and URL and soil moisture, for sandy loam and clay loam soils. Defosse et al. (2003) also found higher quadratic coefficients for estimating critical mechanical parameters with water content on loess and calcareous

soils. Comparison of shape-restricted predictions was also made with quadratic regression to observe the performance of regression modelling.

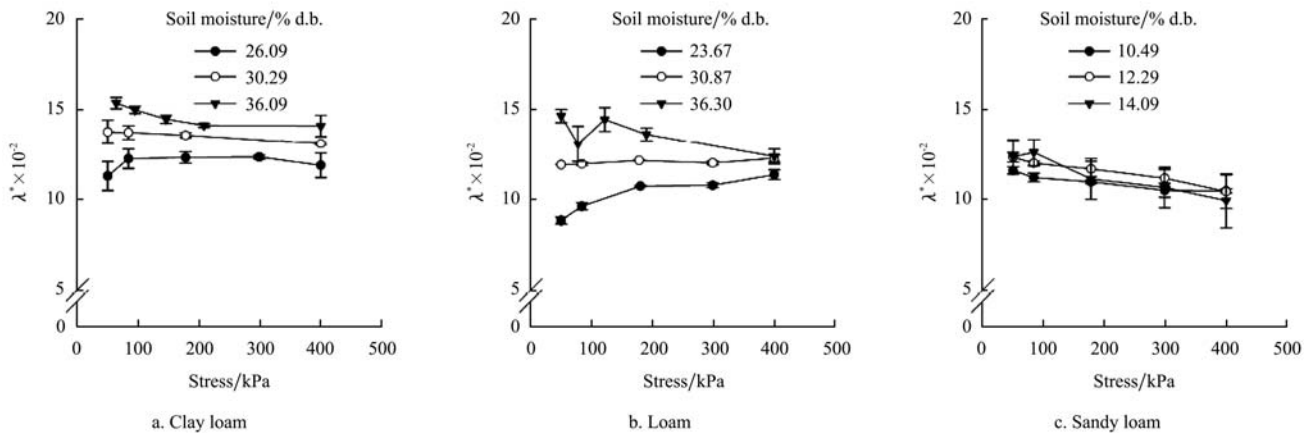


Figure 1 Modified compression index ( $\lambda^* \times 10^{-2}$  (e.g. “5” on vertical axis indicates  $\lambda^* = 0.05$ )) values as a function of maximum applied stress for clay loam, loam and sandy loam soils at three soil moisture levels. Vertical bars indicate standard error values

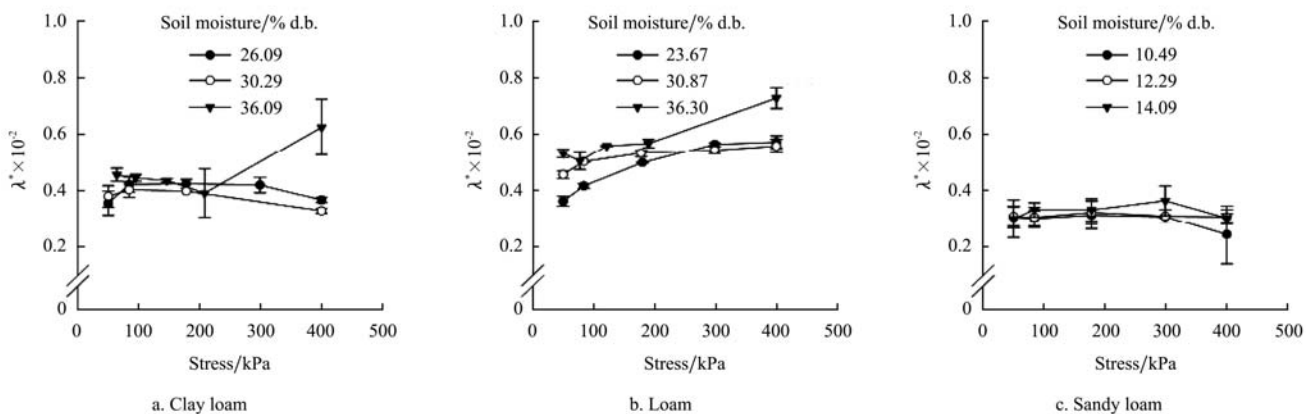


Figure 2 Modified rebound index ( $\kappa^* \times 10^{-2}$  (e.g. “0.2” on vertical axis indicates  $\kappa^* = 0.002$ )) values as a function of maximum applied stress for clay loam, loam and sandy loam soils at three soil moisture levels. Vertical bars indicate standard error values

The shape-restricted model is defined as:

$$\text{Let } y_i = f(x_i) + \beta_1 m_{1i} + \beta_2 m_{2i} + \varepsilon_i, \text{ for } i=1, \dots, n. \quad (8)$$

where,  $x_i$  is maximum applied stress;  $y_i$  is modified compression index or modified rebound index;  $f(x_i)$  is any function belonging to the shape restricted family,  $\beta_1$  and  $\beta_2$  are unknown parameters, and  $\varepsilon_i$  are independently distributed  $N(0,1)$  random errors. The  $m_{ji}$  variables are indicator variables.

$$m_{1i} = \begin{cases} 1 & \text{if dry soil moisture content used for the } i^{\text{th}} \text{ observation} \\ 0 & \text{otherwise} \end{cases}$$

$$m_{2i} = \begin{cases} 1 & \text{if wet soil moisture content used for the } i^{\text{th}} \text{ observation} \\ 0 & \text{otherwise} \end{cases}$$

The constrained set over which we minimize the sum of squared errors is constructed as follows: let  $\theta_i = f(x_i)$  and the monotone nondecreasing constraints can be written as  $(\theta_1 \leq \theta_2 \leq \dots \leq \theta_n)$ . The restriction of  $f$  to the set of convex functions is accomplished by the inequalities

$$\frac{\theta_2 - \theta_1}{x_2 - x_1} \leq \frac{\theta_3 - \theta_2}{x_3 - x_2} \leq \dots \leq \frac{\theta_n - \theta_{n-1}}{x_n - x_{n-1}}$$

Any of these sets of inequalities defines  $m$  half spaces in  $R^n$ , and their intersection forms a closed polyhedral convex cone in  $R^n$ . The cone is designated by  $\mathbf{C} = \{\theta : A\theta \geq 0\}$  for  $m \times n$  constraint matrix  $A$ . Here,  $m = n - 1$  for monotone, nondecreasing convex and  $m = n - 2$  for convex. The nonzero elements of the  $m \times n$  dimensional constraint matrix  $A$  are: for monotone

constraints,  $A_{i,i} = -1$  and  $A_{i,i+1} = 1$  for  $1 \leq i \leq n-1$ . For convex,  $A_{i,i} = x_{i+2} - x_{i+1}$ ,  $A_{i,i+1} = x_i - x_{i+2}$  and  $A_{i,i+2} = x_{i+1} - x_i$  for  $1 \leq i \leq n-2$ . For example, if  $n=5$ , the monotone constraint matrix  $A$  is given by

$$A = \begin{pmatrix} -1 & 1 & 0 & 0 & 0 \\ 0 & -1 & 1 & 0 & 0 \\ 0 & 0 & -1 & 1 & 0 \\ 0 & 0 & 0 & -1 & 1 \end{pmatrix}$$

If  $n = 5$  and the  $x$ -coordinates are equally spaced, the nondecreasing concave and convex constraints are given by the following constraint matrices, respectively:

$$A = \begin{pmatrix} -1 & 2 & -1 & 0 & 0 \\ 0 & -1 & 2 & -1 & 0 \\ 0 & 0 & -1 & 2 & -1 \\ 0 & 0 & 0 & -1 & 1 \end{pmatrix}$$

$$A = \begin{pmatrix} -1 & 2 & -1 & 0 & 0 \\ 0 & -1 & 2 & -1 & 0 \\ 0 & 0 & -1 & 2 & -1 \end{pmatrix}$$

### 2.5.1 Implementation of the shape-restricted regression algorithm

Recall that the ordinary least-squares regression estimator is the projection of the data vector  $y$  on to a lower-dimensional linear subspace of  $R^n$ , whereas the shape-restricted estimator can be obtained through the projection of  $y$  on to an  $m$  dimensional polyhedral convex cone in  $R^n$  (Meyer, 1999). We have the following useful proposition that shows the existence and uniqueness of the projection of the vector  $y$  on a closed convex set (Robertson et al., 1988).

#### Proposition

Let  $C$  be a closed convex subset of  $R^n$ . For  $y \in R^n$  and  $\theta \in C$ , the following properties are equivalent.

- 1)  $\|y - \hat{\theta}\| = \min_{\theta \in C} \|y - \theta\|$
- 2)  $\langle y - \hat{\theta}, \theta - \hat{\theta} \rangle \leq 0$  for all  $\theta \in C$  where the notation  $\langle a, d \rangle = \sum a_i d_i$  refers to the vector inner product of  $a$  and  $d$ .
- 3) For every  $y \in R^n$ , there exists a unique point where  $\hat{\theta} \in C$  satisfies (1) and (2),  $\hat{\theta}$  is said to be the projection of  $y$  onto  $C$ .

Let  $V$  be the linear space vector spanned by  $I = (1, \dots, 1)^T$  for a monotone, nondecreasing convex, and nondecreasing concave, and let  $V$  be linear space spanned by  $I = (1, \dots, 1)^T$  and  $X = (x_1, \dots, x_n)^T$  for convex regression. Note that  $V \in C$  in both cases. The constraint cone can be specified by a set of linearly independent vectors

$$\delta^1, \dots, \delta^n \text{ as } C = \sum_{j=1}^m b_j \delta^j + v : b_j \geq 0 \text{ and } v \in V.$$

where  $m = n-1$  for monotone, nondecreasing concave, nondecreasing convex and  $m = n-2$  for convex. The vectors  $\delta^j$  can be obtained from the formula  $[\delta^1, \dots, \delta^n]^T = (AA^T)^{-1}A$ .

For example, any convex vector  $\theta \in C$  is a nonnegative linear combination of the  $\delta^j$  vectors plus a linear combination of  $I$  and  $X$ .

$$\hat{\theta} = \sum_{j \in J} b_j \delta^j + v$$

The constrained least squares estimate,  $\hat{\theta}$  can be found through Ordinary Least-Squares Regression (OLS) using  $v \in V$  and  $\delta^j$  for  $j \in J$  as regressors. To find the set  $J$  and  $\hat{\theta}$  the mixed primal-dual bases algorithm of Fraser and Massam (1989) was used. Further details on the shape restricted least square estimator are found in Meyer (1999).

The implementation of the algorithm was coded in R, statistical software and the R-code can be obtained upon request from the authors. The code can also be integrated into process flow software packages using user-selected surface response model options.

## 3 Results and discussion

### 3.1 Critical state parameter modified compression index ( $\lambda^*$ )

The uniaxial compressibility of the clay loam and loam soils (Figure 1) showed statistically significant variations with change in soil moisture content. In the clay loam soil, the modified compression index values increased with the increasing soil moisture content for all the stress levels, with the highest values being observed at the wet soil moisture conditions (36.09 % d.b.) (Figure 1a). There was a significant interaction effect of soil moisture content and maximum stress ( $p = 0.006$ ) on the

modified compression index ( $\lambda^*$ ) on the clay loam soil. Within each soil moisture content, there were no statistically significant differences in the modified compression index for higher stress levels ( $\geq 200$  kPa). At low applied stresses, the compression behavior of the clay soil appeared to be more strongly affected by the soil moisture content than at the higher applied stresses. The explanation for the large differences in compressibility at the low stress level may be that at high soil moisture content, the soil water films lubricate the soil particles so they are more easily reoriented into a denser state. A similar observation was made by Holtz and Kovacs (1981) that for wet soil conditions clay soils are generally highly compressible under low applied stress and less compressible under high applied stress.

Generally the influences of soil moisture and maximum applied stress levels on the modified compression index ( $\lambda^*$ ) of the loam soil appeared similar to those of the clay loam soil (Figure 1b). On the loam soil, there was a strong statistical interaction effect of soil moisture and maximum stress on the modified compression index ( $P < 0.0001$ ). At the soil moisture content of 23.67 % d.b., a drier state, the loam soil showed less compression at low applied stress and increased with increasing the applied stress values. The low modified compression index ( $\lambda^*$ ) at this relatively dry soil moisture content was likely associated with the high organic matter content (6.33 %) of the loam soil. As explained by Arvidsson (1998), an increase in organic matter decreases soil compactibility.

As is shown in Figure 1c, the modified compression index values of the sandy loam soil did not vary significantly by soil moisture ( $P = 0.169$ ) and stress ( $P = 0.302$ ). Horn and Lebert (1994) found that coarser textured soils are less compressible than fine textured soils. Unlike the clay loam soil, the sandy loam showed less variability with the change in soil moisture content (10.49 %, 12.29 %, and 14.09 % d.b.). On the sandy loam soil, the modified compression index showed a decreasing trend with an increase in the maximum applied stresses even though the influence was not statistically significant. This may indicate that for soils

with a high sand content, once the soil particles are re-oriented into a denser state under the low maximum applied stress, the soils tend to develop strong resistance for further compression.

### 3.2 Critical state parameter: Modified rebound index ( $\kappa^*$ )

The values of modified rebound index ( $\kappa^*$ ) for clay loam, loam and sandy loam soils are shown in Figure 2a, b, and c. Overall, for the applied stress levels, the clay loam and loam samples tend to rebound more when the soil moisture content was wetter than when the soil was drier. For the loam soil, the interaction of soil moisture content and stress significantly affected the modified rebound index ( $\kappa^*$ ) ( $P < 0.0001$ ). For the clay loam soil, at only the lowest (50 kPa) and highest (400 kPa) stress values, the interaction of soil moisture content and stress significantly affected the modified rebound index ( $\kappa^*$ ) ( $P < 0.0001$ ).

At the intermediate stress levels, the rebound index ( $\kappa^*$ ) was nearly similar for the three soil moisture contents. The loam soil showed high rebound behavior with a modified rebound index values ( $\kappa^* \times 10^{-2}$ ) range of -0.300 to -0.005, i.e. the  $\kappa^*$  range is from -0.00300 to -0.00005, and were higher than those for the sandy loam and clay loam soils. The strong rebound behavior of the loam soil could be associated with the high soil organic matter content (6.33 %). The loam soils in Sheeb, in the eastern coastal plains of Eritrea, are situated in seasonal river beds (locally called *wadis*) and annually receive an average of 143 t ha<sup>-1</sup> of sediments and organic materials (Tesfai and Streck, 2002). Similar to the modified compression index behavior, rebound characteristics of the sandy loam soil were generally low and not as sensitive to soil moisture variations as for the clay loam and loam soils.

The values of the modified rebound index were smaller than the values of modified compression index for all of the soil types and treatment factors (soil moisture content and maximum stress). Averaged by soil moisture content and stress levels, the ratio of  $\lambda^*/\kappa^*$  for clay loam, loam and sandy loam soils were  $32.75 \pm 3.21$ ;  $23.00 \pm 2.68$ ; and  $36.46 \pm 3.54$ , respectively. The

rebound index was approximately 3%-4% of the compression index.

The compression and rebound index values obtained on the studied soils were compared to those from other works (Table 3). It appeared that the critical state parameter values varied depending on the testing methods used and the quality of samples (undisturbed or remolded). The compression and rebound index values computed from the uniaxial compression stress on the clay loam, loam and sandy loam soils from this study were overall within the range of values from triaxial tests

of similar soil types and range of soil moisture contents. The compression and rebound indices computed from triaxial test data on undisturbed soil samples tend to have higher values than the values from uniaxial compression on remolded soil samples. For finite element analysis, it appeared that quick uniaxial testing could provide values of the critical state parameters comparable to triaxial testing which employs rigorous stress path loadings but is time-consuming in sample preparation and conducting the experiment.

**Table 3 Values of compression index ( $\lambda$ ) and rebound index ( $\kappa$ ) from different authors <sup>[1]</sup>**

	Soil type	Soil Moisture (% d.b.)	Testing method	$\lambda(\times 10^{-2})$ <sup>[2]</sup>	$\kappa(\times 10^{-2})$ <sup>[2]</sup>
Petersen (1993) (Tastrup and Marum soils from Denmark)	Sandy loam	2 – 25	Triaxial on remolded samples	8 – 18	1.1 – 1.6
	Loam	10 – 27		13 – 24	1.2 – 1.9
O'Sullivan and Robertson (1996) ( <i>Eutric Cabisol</i> and <i>Gleysol</i> from Scotland)	Sandy loam	13 – 19	Triaxial in undisturbed samples	0.3 – 16	0.17 – 0.71
	Clay loam	18 – 25		2.3 – 19	0.41 – 1.28
Poodt M.P. et al. (2003) (Lobith loam soil from Netherlands)	Loam	19 – 23	Uniaxial compression on remolded samples	5 – 8	0.2 – 0.3
Tekeste et al. (2009) ( <i>Lixisols</i> , <i>Leotosols</i> and <i>Fluvisols</i> from Eritrea)	Sandy loam	11 – 14	Uniaxial compression on remolded soils	10 – 12	0.2 – 0.4
	Loam	24 – 36		9 – 13	0.4 – 0.7
	Clay loam	26 – 34		0.11 – 0.16	0.3 – 0.5

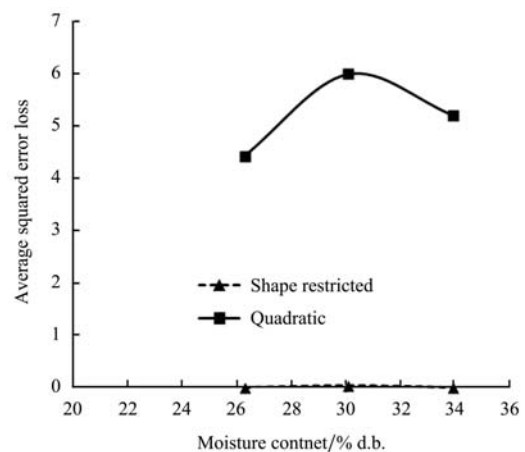
**Note:** <sup>[1]</sup> To compared similar index values from the different authors, the compression index ( $\lambda$ ) and rebound index ( $\kappa$ ) in this table refer to the index values computed from void ratio ( $e$ ) and logarithmic normal stress ( $\ln(p)$ ) relationships.

<sup>[2]</sup> For example, a value of " $\lambda(\times 10^{-2})$ " of 8 indicates  $\lambda = 0.08$  and a value of " $\kappa(\times 10^{-2})$ " of 1.1 indicates  $\kappa = 0.011$ .

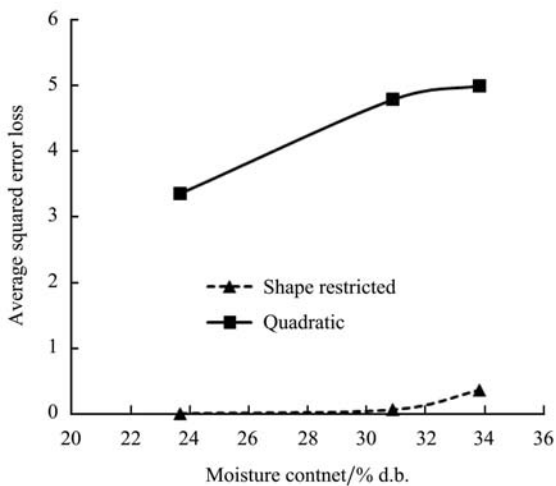
**3.3 Shape-restricted vs. quadratic regression fitting of critical state parameters as a function of maximum stress**

The shape-restricted regressed models that assumed the modified compression and rebound indices attained certain shapes, fitted better than quadratic regression models in all cases. The shape-restricted regression had smaller Average Squared Error Loss (ASEL) than a quadratic regression for the modified compression index (Figure 3) and modified rebound index (Figure 4). As is shown in Figures 3 and 4, soil mechanical parameters generally were predicted better (lower ASEL) at the dry soil moisture contents than at the wet soil moisture contents for all soil types. The parameter estimates for the quadratic regression of the modified compression index and the modified rebound index are shown in Table 4 and Table 5, respectively. Across the soil moisture contents, the higher order terms of the quadratic

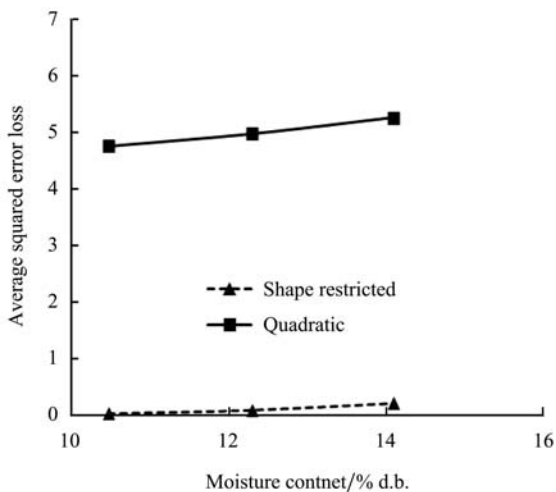
regression were not significant ( $P > 0.05$ ) for both the modified compression and rebound index models. In curve fitting, quadratic regression was applied with the intercept forced to be zero because the values of the mechanical parameters are zero when the applied stress level is zero.



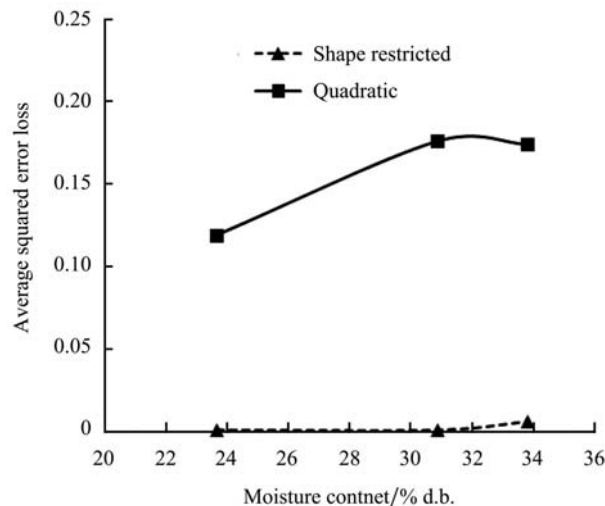
a. Clay loam



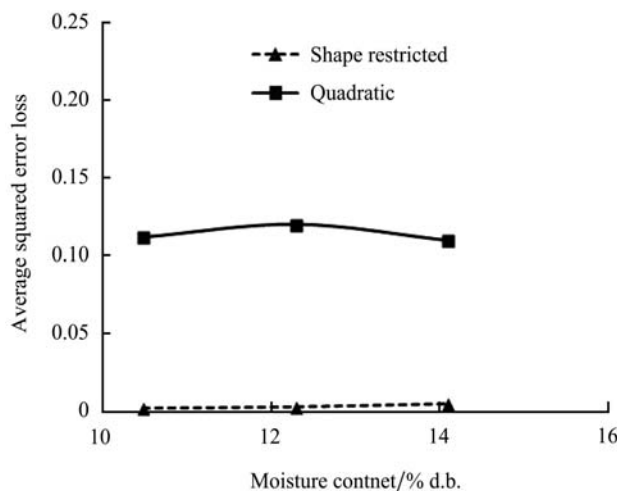
b. Loam



c. Sandy loam



b. Loam



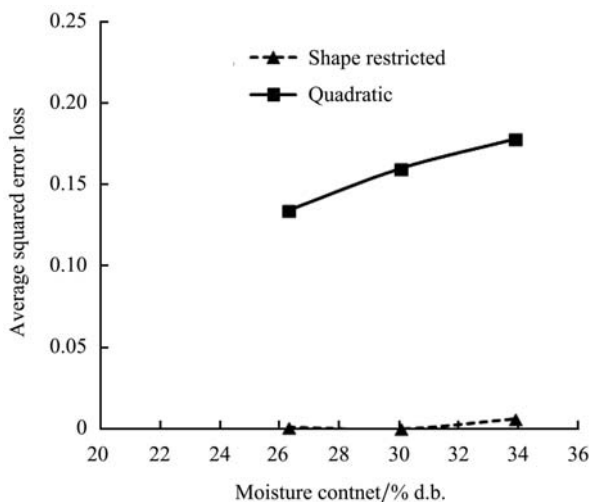
c. Sandy loam

Figure 3 Average Squared Error Loss (ASEL) of shape-restricted regression and quadratic regression for predicting the modified compression index ( $\lambda^*$ ) for clay loam, loam and sandy loam soils

Figure 4 Average Squared Error Loss (ASEL) of shape-restricted regression and quadratic regression for predicting the modified rebound index ( $\kappa^*$ ) for clay loam, loam and sandy loam soils

**Table 4 Coefficient estimates of the quadratic regression for clay loam, loam and sandy loam soils at three soil moisture contents with the modified compression index ( $\lambda^* \times 10^{-2}$ ) as a dependent variable and maximum applied stress as an independent variable**

		Soil Moisture (% d.b.)					
		26.29		30.07		33.9	
$X =$	maximum applied stress	Parameter Estimate	P-Value	Parameter Estimate	P-Values	Parameter Estimate	P-Value
$X$		0.1285	0.02	0.1596	0.08	0.158	0.019
$X^2$		-0.0003	0.07	-0.0003	0.13	-0.0003	0.05



a. Clay loam

Loam Soil

$X =$ maximum applied stress	Soil Moisture (% d.b.)					
	23.67		30.87		33.82	
	Parameter Estimate	P-Value	Parameter Estimate	P-Value	Parameter Estimate	P-Value
$X$	0.1029	0.02	0.1263	0.04	0.1467	0.03
$X^2$	-0.0002	0.07	-0.0003	0.09	-0.0003	0.05

Sandy Loam Soil

$X =$ maximum applied stress	Soil Moisture (% d.b.)					
	10.47		12.29		14.09	
	Parameter Estimate	P-Value	Parameter Estimates	P-Value	Parameter Estimates	P-Value
$X$	0.1180	0.04	0.1277	0.04	0.1271	0.05
$X^2$	-0.0002	0.10	-0.0003	0.09	-0.0003	0.10

**Table 5 Coefficient estimates of the quadratic regression for clay loam, loam and sandy loam soils at three soil moisture contents with the modified rebound index ( $\kappa^* \times 10^{-2}$ ) as a dependent variable and maximum applied stress as an independent variable**

Clay loam soil

$X =$ maximum applied stress	Soil Moisture (% d.b.)					
	26.29		30.07		33.9	
	Parameter Estimate	P-Value	Parameter Estimate	P-Value	Parameter Estimate	P-Value
$X$	0.00444	0.02	0.00469	0.07	0.00411	0.04
$X^2$	-0.00001	0.05	-0.00001	0.11	-0.00001	0.14

Loam soil

$X =$ maximum applied stress	Soil Moisture (% d.b.)					
	23.67		30.87		33.82	
	Parameter Estimate	P-Value	Parameter Estimate	P-Value	Parameter Estimate	P-Value
$X$	0.00446	0.01	0.00530	0.03	0.00560	0.02
$X^2$	-0.00001	0.05	-0.00001	0.07	-0.00001	0.06

Sandy loam soil

$X =$ maximum applied stress	Soil Moisture (% d.b.)					
	10.47		12.29		14.09	
	Parameter Estimate	P-Value	Parameter Estimate	P-Value	Parameter Estimate	P-Value
$X$	0.00341	0.03	0.00332	0.03	0.00359	0.02
$X^2$	-0.00001	0.05	-0.00001	0.08	-0.00001	0.05

**3.4 Volumetric plastic strain for linear hardening rule of Cam-clay model**

For the piecewise linear form of the clay plasticity

hardening rule option in the ABAQUS Cam-clay model, tabular data of plastic natural volumetric strains and yield stress values can be estimated from the oedometer data (ABAQUS, 2004). Using the initial stress, the strain, the compression index and rebound index values, the plastic (irrecoverable) volumetric deformation were computed from the oedometer test data using Equations (9) and (10).

$$\bar{\varepsilon}_v = \ln \left( \frac{v_i}{v_o} \right) \tag{9}$$

where  $\bar{\varepsilon}_v$  = total natural volumetric strain;  $v_i$  = specific volume at the maximum stress value; and  $v_o$  = specific volume at pre-load stress (10 kPa). The elastic natural volumetric strain values were also computed similarly with specific volume values from the maximum stress and the lowest stress value (Equation (10)).

$$\bar{\varepsilon}_{v_e} = \ln \left( \frac{v_i}{v_e} \right) \tag{10}$$

where  $\bar{\varepsilon}_{v_e}$  = elastic natural volumetric strain;  $v_i$  = specific volume at the maximum stress value; and  $v_e$  = specific volume at lowest rebound stress (5 kPa).

The plastic natural volumetric strain values ( $\bar{\varepsilon}_{v_p}$ ) were then obtained by subtracting the elastic natural volumetric strain values from the total natural volumetric strain values ( $\bar{\varepsilon}_{v_p} = \bar{\varepsilon}_v - \bar{\varepsilon}_{v_e}$ ).

As is shown in Figure 5, the plastic (irrecoverable) volumetric strain values from the maximum applied stresses on the clay loam soil were generally greater than the values on the sandy loam and loam soils.

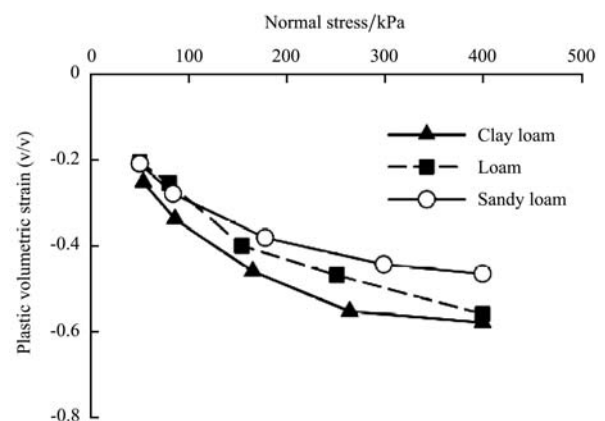


Figure 5 Plastic natural volumetric strain and normal stress relationships for clay loam, loam and sandy loam soils

On weakly structured soils the maximum applied stress in a uniaxial compression test approximates the pre-consolidation stress ( $\sigma_{pc}$ ) which is often estimated by using the Casagrande method and represents the transition from elastic to plastic regions in the stress-strain relationship (Mosaddeghi et al., 2007). The results show that for accurately modeling compaction on unsaturated soils, for loading from wheeling for which the major principal stress,  $\sigma_1$ , is the dominant stress, the best fitted shape-restricted regression technique or plastic-yield stress in Figure 5 can be successfully used to generate modified Cam-clay plastic model parameters.

#### 4 Conclusion

Unsaturated samples of agricultural soils were subjected to quick uniaxial compression tests to measure modified Cam-clay soil model parameters of modified compression ( $\lambda^*$ ) and rebound ( $\kappa^*$ ) indices and investigate their behaviors with variations in soil type, soil moisture content and the maximum stress applied. The parameters showed variation with soil types, soil moisture contents and maximum applied stress. It was found that on a clay loam soil higher compressibility was observed at lower stress levels and wet moisture conditions (-10 kPa soil moisture potential) than at higher stress levels. The loam soil had similar compression and rebound characteristics to the clay loam. Soil moisture did not significantly affect the Cam-clay parameters on a

sandy loam soil. The sandy loam soil showed the lowest values of modified compression index ( $\lambda^*$ ) and modified rebound index ( $\kappa^*$ ). On average, the modified compression index ( $\lambda^*$ ) was about 23 to 36 times the modified rebound index ( $\kappa^*$ ). The shape-restricted regression technique was presented to predict the modified Cam-clay model parameters as a function of pre-consolidation stress at different levels of soil moisture content. The shape-restricted method provided more accurate estimates at reduced average squared error loss and this demonstrated the applicability of the method for prediction of model parameters. The benefit of the shape-restricted regressions is that they can provide a flexible fit to the data, while polynomial regressions require the fixed forms of the underlying distribution function.

#### Acknowledgments

The study was done at the Soil Technology Group of Wageningen University, the Netherlands. The authors thank Ing. B. Kroesbergen, a staff at Soil Technology group, for training in soil testing methods. We are thankful also to the financial support from NUFFIC-MHO and University of Asmara, Eritrea. The authors would like to thank anonymous referees and editor for their valuable comments and discussions on the topic that improved the exposition of the paper.

#### References

- ABAQUS, Version 6.4. 2004. Abaqus theory manual. ABAQUS, Inc. USA.
- Adams, B. A., and D. Wulfsohn. 1998. Critical-state behaviour of an agricultural soil. *Journal of Agricultural Engineering Research*, 70(4): 345-354.
- Al-Adawi, S. S., and R. C. Reeder. 1996. Compaction and subsoiling effects on corn and soybean yields and soil physical properties. *Transactions of the ASAE*, 39(5): 1641-1649.
- Arvidsson, J. 1998. Influence of soil texture and organic matter content on bulk density, air content, compression index and crop yield in field and laboratory compression experiments. *Soil and Tillage Research*, 49(1): 159-170.
- Atkinson, J. H., and P. L. Bransby. 1978. The mechanics of soils, An introduction to critical soil mechanics. London: McGraw Hill.
- Bailey, A. C., and C. E. Johnson. 1989. A soil compaction model for cylindrical stress state. *Transactions of the ASAE*, 32(3): 822-825.
- Barlow, R. E., and H. D. Brunk. 1972. The isotonic regression problem and its dual. *Journal of the American Statistical Association*, 67(337): 140-147.
- Brinkgreve, R. B., and P. A. Vermeer. 1998. PLAXIS Finite Element Code for Soil and Rock Analysis. Version 7. Rotterdam, the Netherlands: Balkema.
- Chiroux, R. C., W. A. Foster, C. E. Johnson, S. A. Shoop, and R. L. Raper. 2005. Three-dimensional finite element analysis of

- soil interaction with a rigid wheel. *Applied Mathematics and Computation*, 162(2): 707-722.
- Défossez, P., G. Richard, H. Boizard, and M. F. O'Sullivan. 2003. Modeling change in soil compaction due to agricultural traffic as function of soil water content. *Geoderma*, 116(1): 89-105.
- FAO-UNESCO. 1988. Soil map of the world, revised legend with correction. World soil resources report 60. Rome, Italy: FAO.
- Fielke, J. M. 1999. Finite element modeling of the interactions of cutting edge of tillage implements with soil. *Journal of Agricultural Engineering Research*, 74(1), 91-101.
- Fraser, D. A. S., and H. Massam. 1989. A mixed primal-dual bases algorithm for regression under inequality constraints. Application to concave regression. *Scandinavian Journal of Statistics*, 16(1): 65-74.
- Hamza, M. A., and W. K. Anderson. 2005. Soil compaction in cropping systems: A review of the nature, causes and possible solutions. *Soil and Tillage Research*, 82(2): 121-145.
- Hillel, D. 1998. Environmental soil physics. San Diego, Calif.: Academic Press.
- Holtz, R. D., and W. D. Kovacs. 1981. An introduction to geo-technical engineering. Englewood Cliffs, N.J: Prentice Hall.
- Horn, R., and M. Lebert. 1994. Soil compactability and compressibility. In Soil compaction in crop production (Soane B D; van Ouwerkerk C, eds), pp 45 – 69. Amsterdam: Elsevier.
- Koolen, A. J. 1974. A method for soil compactability determination. *Journal of Agricultural Engineering Research*, 19(3): 271-278.
- Koolen, A. J. 1987. Deformation and compaction of elemental soil volumes and effects on mechanical soil properties. *Soil and Tillage Research*, 10(1): 5-19.
- Koolen, A. J. 1994. Mechanics of soil compaction. In: Soil Compaction in Crop Production (Soane B D; van Ouwerkerk C, eds), pp 23–44. Amsterdam: Elsevier.
- Koolen, A. J., and H. Kuipers. 1983. Agricultural soil mechanics. Berlin: Springer-Verlag.
- Kirby, J. M., and M. F. O'Sullivan. 1997. Critical state soil mechanics analysis of the constant cell volume triaxial test. *European Journal of Soil Science*, 48(1): 71-78.
- Kruskal, J. B. 1964. Multidimensional scaling by optimizing goodness of fit to a nonmetric hypothesis. *Psychometrika*, 29(1): 1-27.
- Lal, R., and B. A. Stewart. 1994. Land Degradation. Advances in Soil Science. Vol. 11, New York: Springer.
- Meyer, M. C. 1999. An extension of the mixed primal–dual bases algorithm to the case of more constraints than dimensions. *Journal of Statistical Planning and Inference*, 81(1): 13-31.
- Meyer, M. C., and D. Habtzghi. 2011. Nonparametric estimation of density and hazard rate functions with shape restrictions. *Journal of Nonparametric Statistics*, 23(2): 455-470.
- Ministry of Agriculture (MoA); University of Asmara (UoA). 1998. Rehabilitation of degraded lands (2nd ed.), Eritrea.
- Mosaddeghi, M. R., A. J. Koolen, A. Hemmat, M. A. Hajabbasi, and P. Lerink. 2007. Comparisons of different procedures of pre-compaction stress determination on weakly structured soils. *Journal of Terramechanics*, 44(1): 53-63.
- Mouazen, A. M., and M. Neményi. 1999. Finite element analysis of subsoiler cutting in non-homogeneous sandy loam soil. *Soil and Tillage Research*, 51(1): 1-15.
- Obozinski, G., G. Lanckriet, C. Grant, M. I. Jordan, and W. S. Noble. 2008. Consistent probabilistic outputs for protein function prediction. *Genome Biology* (Suppl 1), S6.
- O'Sullivan, M. F., and E. A. G. Robertson, 1996. Critical state parameters from intact samples of two agricultural topsoils. *Soil and Tillage Research*, 39(3): 161-173.
- O'Sullivan, M. F., J. K. Henshall, and J. W. Dickson. 1999. A simplified method for estimating soil compaction. *Soil and Tillage Research*, 49(4): 325-335.
- Petersen, C. T. 1993. The variation of critical - state parameters with water content for two agricultural soils. *Journal of Soil Science*, 44(3): 397-410.
- Poodt, M. P., A. J. Koolen, and J. P. Van der Linden. 2003. FEM analysis of subsoil reaction on heavy wheel loads with emphasis on soil preconsolidation stress and cohesion. *Soil and Tillage Research*, 73(1): 67-76.
- Radcliffe, D. E., L. T. West, R. L. Clark, G. Manor, G. W. Langdale, and R. R. Bruce. 1989. Effect of traffic and in-row chiseling on mechanical impedance. *Soil Science Society of America Journal*, 53(4): 1197-1201.
- Raper, R. L. 2005. Agricultural traffic impacts on soil. *Journal of Terramechanics*, 42(3): 259-280.
- Robertson, T., F. T. Wright, R. L. Dykstra, and T. Robertson. 1988. Order restricted statistical inference. Hoboken, N.J.: Wiley.
- Roscoe, K. H., A. Schofield, and C. P. Wroth, 1958. On the yielding of soils. *Geotechnique*, 8(1): 22-53.
- Schell, M. J., and B. Singh. 1997. The reduced monotonic regression method. *Journal of the American Statistical Association*, 92(437): 128-135.
- Smith, C. W., M. A. Johnston, and S. Lorentz. 1996. Assessing the compaction susceptibility of South African forestry soils. I. The effect of soil type, water content and applied pressure on uniaxial compaction. *Soil and Tillage Research*, 41(1): 53-73.
- Soane, B. D., and C. Van Ouwerkerk. 1994. Soil compaction in crop production. Developments in Agricultural Engineering. Amsterdam: Elsevier.

- Söhne, W. 1958. Fundamentals of pressure distribution and soil compaction under tractor tires. *Agricultural Engineering*, 39(5): 290.
- Tesfai, M., and G. Sterk. 2002. Sedimentation rate on spate irrigated fields in Sheeb area, eastern Eritrea. *Journal of Arid Environments*, 50(1): 191-203.
- Tekeste, M. Z. 1999. Soil compaction assessment of Eritrean soils under agricultural mechanization. M.Sc. Thesis. Wageningen University, Wageningen, The Netherlands.
- Upadhyaya, S. K., U. A. Rosa, and D. Wulfsohn. 2002. Application of the finite element method in agricultural soil mechanics. In *Advances in Soil Dynamics, Vol. 2*, ed. S.K. Upadhyaya, W.J. Chancellor, J.V. Perumpral, R.L. Schafer, W.R. Gill, and G.E. Vanden Berg, 117-153. St. Joseph, Mich.: ASAE.
- Van den Akker, J. J. H., J. Arvidsson, and R. Horn. 2003. Introduction to the special issue on experiences with the impact and prevention of subsoil compaction in the European Union. *Soil and Tillage Research*, 73(1): 1-8.
- Wiermann, C., D. Werner, R. Horn, J. Rostek, and B. Werner. 2000. Stress/strain processes in a structured unsaturated silty loam Luvisol under different tillage treatments in Germany. *Soil and Tillage Research*, 53(2): 117-128.
- Weisberg, S. 2005. *Applied Linear Regression*. Hoboken, N.J.: Wiley.
- Wood, M. D. 1990. *Soil behavior and critical state soil mechanics*. Cambridge, UK: Cambridge University Press.
- Wulfsohn, D., and B. A. Adams. 2002. Elastoplastic soil mechanics - Part II, Critical state soil mechanics for unsaturated agricultural soils. Chapter 1, In *Advances in Soil Dynamics, Vol. 2*, ed. S.K. Upadhyaya, W.J. Chancellor, J.V. Perumpral, R.L. Schafer, W.R. Gill, and G.E. Vanden Berg, 71-116. St. Joseph, Mich.: ASAE.
- Zheng, Z., H. Zha, and G. Sun. 2008. Query-level learning to rank using isotonic regression. In *Communication, Control, and Computing, 2008 46th Annual Allerton Conference on IEEE*, 1108-1115.
- ZWICK Universal material testing machine. 1998. Ulm, Germany: Zwick Gmbh & Co. KG.